Local investigation of thin insulating barriers incorporated in magnetic tunnel junctions

T. Dimopoulos,[a] V. Da Costa, C. Tiusan, and K. Ounadjela
Institut de Physique et Chimie des Materiaux de Strasbourg (IPCMS), 23 rue du Loess, F-67037 Strasbourg Cedex, France

H. A. M. van den Berg
Siemens AG, ZT MF1, Paul Gossenstrasse 100, Erlangen D-91052, Germany

In this work we study properties of very thin insulating Al oxide films, used as barriers in magnetic tunnel junctions. For the small barrier thicknesses required for technological applications (~10 Å), the presence of pinholes (direct contact between the ferromagnetic metals through the barrier), or oxidation inhomogeneities, are the major factors for vanishing of the tunnel magnetoresistance effect. We have produced and characterized very thin, pinhole-free Al oxide layers, incorporated in magnetic tunnel junctions. The transport properties of the different barriers were analyzed by barrier impedance scanning microscopy and were correlated with the magnetotransport properties of the patterned microsized junctions. © *2001 American Institute of Physics.* [DOI: 10.1063/1.1361052]

After the discovery of large tunnel magnetoresistance (TMR) at room temperature,[1] many potential applications such as magnetic sensors, magnetic random access memories, and heads, have emerged using magnetic tunnel junctions (MTJs), which consist of a thin insulating layer (*I*) sandwiched between two ferromagnetic (FM) metals. Especially for high storage density magnetic heads, a low resistance–area product of the MTJ is requried, on the order of $100\Omega\times(\mu\mathrm{m})^2$. This serves to increase the TMR signal-to-noise ratio, as well as to decrease the time constant *RC* involved in the reading and writing processes, where *R* is the resistance of the junction and *C* its capacitance. The insulating tunnel barrier employed in the MTJ stack has to be of very high quality in terms of large scale homogeneity of its parameters (thickness and height). Aluminum oxide has been proven the easiest tunnel barrier to fabricate. Nevertheless, good control and optimization of the deposition and oxidation techniques are required. For highly conducting tunnel barriers the above requirement is more difficult to be fulfilled. The reason is that the interfacial phenomena become increasingly significant compared to the bulk phenomena as the thickness of the oxide layer reduces. This work investigates the physical properties of highly conducting thin Al oxide insulating layers (thickness of Al film before oxidation from 5 to 12 Å). The main goal is to shed light on the mechanisms of tunneling by correlating the magnetotransport properties of patterned junctions with the nanometric-scale transport properties of the tunnel barrier, using barrier impedance scanning microscopy (BISM).[2]

The multilayers were fabricated by dc and rf magnetron sputtering on Si(111) wafers. First, a buffer trilayer of Cr(1.8 nm)/Fe(6 nm)/Cu(30 nm) is sputtered. Upon the buffer, an artificial antiferromagnet of CoFe(1.5 nm)/Ru(0.8 nm)/CoFe(2.5 nm) serves as the magnetically hard subsystem.[3,4] A CoFe(1 nm)/Fe(6 nm) bilayer is used as soft (detection) subsystem. Between the hard and the soft system the Al oxide barrier is formed. A metallic Al film is initially sputtered and subsequently oxidized within an rf Ar/O_2 plasma. Etching and oxidation of the Al film take place at the same time on the surface of the sample. If the etching rate caused by the Ar is larger than the oxidation rate of the metal, the surface stays metallic. In the opposite case, the oxidation progresses until the oxidation rate, which decreases with increasing oxide thickness, becomes equal to the etching rate. We can thus expect a regime where the thickness of the oxide remains constant. Details on this technique can be found in Refs. 5 and 6. Finally, the multilayer stack is capped with Cu(20 nm)/Cr(3 nm). UV photolithography is used to pattern the junctions in nominal areas of 3×3 up to $20\times20\ \mu\mathrm{m}^2$. The transport measurements are realized with a four-point technique. With the scaling of the resistance inversely with the area of the junction, the almost constant TMR [regardless of the junction's size and the calculated low resistivity of the bottom Cu electrode ($<0.3\ \Omega$)], allow us to exclude any artificial geometrical enhancement of the TMR due to inhomogeneous current flow through the junction area. The above applies even for the lowest resistance junctions measured in this study.

Information on the barriers used in this study are collected in Table I. It is noted here that the AlO_x thickness is expected to be larger by about 30% than that of the initially deposited metallic Al film, as verified by the TEM images of the barrier.

TABLE I. Description of studied barriers.

Barrier	Al thickness d_{Al} (Å)	Oxidation time t_{ox}
B1	12	45
B2	10	35
B3	8	35
B4	6	30
B5	5	30

[a]Author to whom correspondence should be addressed; electronic mail: thdimop@ipcms.u-strasbg.fr

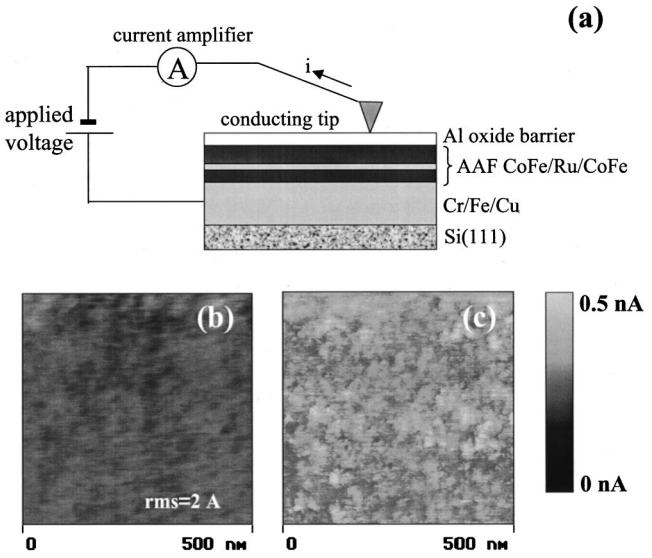

FIG. 1. (a) Schematic of the BISM with the layered structure. (b) and (c) Topographic and current map image, respectively, acquired by BISM.

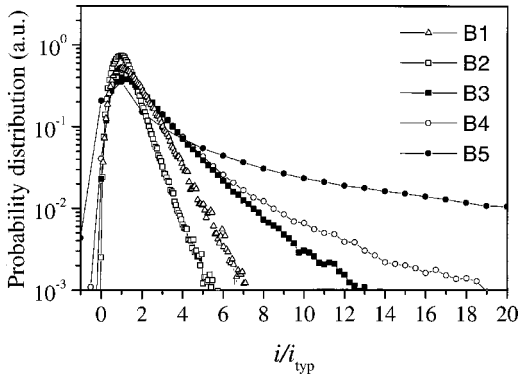

FIG. 2. The probability distribution vs the normalized current density for the studied barriers using BISM.

The quality of the barriers has been verified by various techniques. Magnetometry measurements showed no direct coupling between the FM electrodes adjacent to the barrier, verifying the continuity of the oxide layer. TEM also revealed large scale continuity and correlated roughness of the oxide layer as well as good quality metal/oxide interfaces. The bottom FM electrode/oxide interface was probed by XPS, and showed no significant oxidation of the FM electrode for barriers B1 and B2, Although for the systems employing barriers B3, B4, and B5 increasingly significant overoxidation of the barrier is observed.

For the BISM experiments, the deposition of the multilayers has been stopped exactly after the formation of the tunnel barrier. BISM uses a conducting AFM tip to simultaneously acquire the topographic and the current map image of the scanned barrier surface, when a bias is applied between the tip and the ferromagnetic metal (typically 1.5 V), which lies beneath the insulating barrier. A schematic of the microscope with the layered structure used is depicted in Fig. 1(a). The significance of this technique is that it can map at the nanometric scale the local current transmitted through the barrier.[2] Thus, any spatial fluctuations of the local current density, arising from the distribution of barrier thickness and/or height over the scanned area, can be probed and quantified.

Each sample listed in Table I has been analyzed using this technique. The scanned images were captured in $500 \times 500\,\mathrm{nm}^2$ size (512×512 pixels). In Figs. 1(b) and 1(c) the topographic and current map images, respectively, are presented for a system employing barrier B2. From the current map images, the probability distribution of the current intensity is acquired. We will call the most probable value of the current i_{typ}. The current density for the scanned area of the barrier gives values in the same order of magnitude as for the corresponding patterned junctions. This is additional evidence that the experimental setup does not alter the intrinsic properties of the barrier and that it can probe with sufficient accuracy the local transport characteristics.

Topographic profiles of the scanned areas show no correlation with the current map images [Figs. 1(b) and 1(c)]. In Fig. 2 we plot the normalized probability distribution for the quantity i/i_{typ}, for all the tunnel barriers (we use the quantity i/i_{typ} instead of i, in order to compare the barrier fluctuations in the same scale and to exclude any possibility of artifacts that may arise from the conducting tip). Interestingly, the probability distribution broadens when the barrier becomes thinner, while its tail extends to higher i/i_{typ} values.

The mean value $\langle i/i_{typ} \rangle$ is of great importance as it characterizes the homogeneity of the tunnel barriers on junctions. At higher disorder the position of the mean $\langle i/i_{typ} \rangle$ is shifted far away from the distribution maximum (a perfect system without any fluctuation shows $\langle i/i_{typ} \rangle = 1$). Calculating the above quantity for each barrier case, we get $\langle i/i_{typ} \rangle$ equal to the values presented in Table II. The larger the deviation of the above quantity from unity, the larger the disorder in the barrier, and the more significant the contribution of the highly conducting sites (hotspots) of the distribution's tail on the total current. It is the case for barriers B4 and B5 (thinnest barriers) which presents more pronounced tails (see Fig. 2). The hotspots are expected to correspond in a lower barrier height or barrier thickness and, thus, to be detrimental for the TMR effect. We note here that in no case did the BISM experiment show the existence of pinholes. Even the highest conducting sites, when probed by the tip, gave a nonlinear current–voltage $I-V$ characteristic, indicative of tunneling mechanisms. In the following paragraphs we will try to find a correlation between the above results and the measured characteristics of the corresponding patterned tunnel junctions.

TABLE II. Properties of the barriers.

Barrier	$R \times A$ k$\Omega \times (\mu\mathrm{m})^2$	d_{AlO_x} (Å)	φ (eV)	$\langle i/i_{typ} \rangle$	TMR (%)
B1	35	9.7	2.6	1.2	24
B2	6	8.9	1.5	1.1	25.5
B3	1.3	11.2	0.75	2.3	14
B4	0.2	—	—	3	7
B5	0.08	—	—	10	0.1

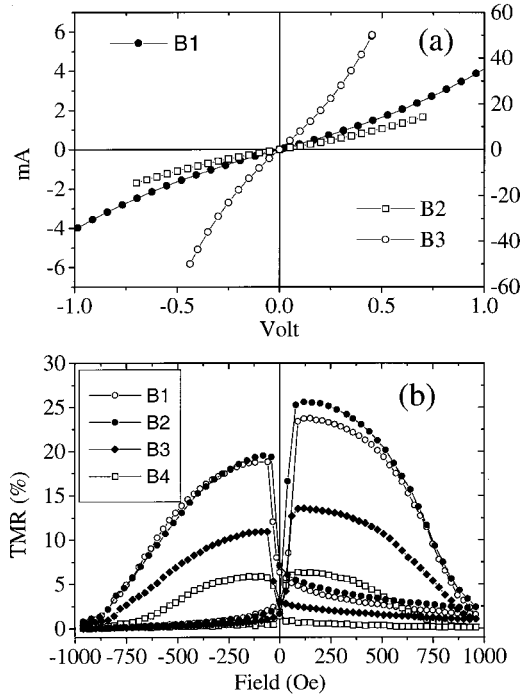

FIG. 3. (a) $I-V$ curves for junctions with barriers B1 (left scale), B2 and B3 (right scale). (b) TMR loops for junctions employing barriers B1, B2, B3, and B4.

Identical barriers to the ones used for BISM were incorporated in MTJs. By fitting the junctions' $I-V$ curves [Fig. 3(a)] to the formula of Simmons we obtained the values of the barrier height φ and thickness d shown in Table II. For junctions with thinner barriers the acquisition of an $I-V$ at such an extent that safe fitting could be realized was not possible. The first significant fact is the decrease of the barrier height as the nominal thickness of the barrier is decreased. Specifically, the barrier height drops from 2.6 eV for B1 to 0.75 eV for B3. The TMR ratio for junctions employing B1 and B2 have comparable values of 24% and 25.5%, respectively [Fig. 3(b)], while it drops to 14% for MTJs with B3 and 7% for B4 [Fig. 3(b)]. The tunnel magnetoresistance effect vanishes for junctions incorporating barrier B5. We note here that the extracted thickness for B3 is shown to be larger than this of B1 and B2. This most probably has to do with the overoxidation of the barrier, as already shown by the XPS experiment.

We believe that a strong correlation exists between the data acquired from BISM and the eventual magnetotransport properties of patterned junctions. A correlation which poses the issue of the disorder effects in the insulator. For example, impurities, defects, or even structural disorder can create localized electronic states within the gap of the insulator, favoring resonant tunneling. Intermixing between the ferromagnetic metal forming the electrodes of the junction and Al can also degenerate the junction's interfaces and create interfacial energy states. For usual oxide formation procedures, significant disorder originates from the oxidation of the metallic Al layer. The optimization of the oxidation time for each Al thickness is very difficult and under-or overoxidation of the barrier is in many cases possible. The oxidation of the bottom CoFe electrode can also give rise to a rougher interface with the AlO_x, extending over 1 or 2 monolayers. This small ''wavelength'' roughness is not correlated with the upper interface and thus accounts for thickness fluctuations in the barrier. It is logical to assume that by decreasing the barrier thickness, the interfacial phenomena become increasingly important, up to a point when they can dominate over the bulk properties of the oxide. This suggested mechanism is supported by the close dependence that we observe between the $\langle i/i_{\mathrm{typ}}\rangle$ and the TMR value (Table II). The highest is the system's disorder, the lowest is the magnetoresistive effect. For extremely disordered systems (barrier B5) the TMR is vanishing. The tunneling process is mainly determined by the highly conducting ''channels'' connecting the two FM metals through the insulator. These formations assist the tunneling, reducing effectively the barrier height. As the barrier becomes thinner the mean value of the current is shifted further away from the distribution's maximum, denoting the dominant tunneling contribution from a few configurations providing high conductance and a low magnetoresistive effect.

In conclusion, in this article we have underlined the correlation between the local transport properties of the tunnel barrier with the quantities deduced from measuring patterned micronic junctions (TMR, barrier height, and thickness). It is shown that the highly conducting sites of the barrier, corresponding to the tail of the current distribution measured by BISM, become increasingly important when reducing the barrier thickness. These ''defective'' sites effectively reduce the barrier height and are detrimental for the TMR signal.

The authors would like to thank Dr. M. Hehn and Dr. Y. Henry for illuminating discussions and Dr. C. Meny, M. Acosta, G. Wurtz, and G. Ehret for experimental support. This work was partially supported by the European Community Brite Euram project 'Tunnelsense' (Grant No. BRPR98-0657) and the Training and Mobility of Researchers program of the EC through the Dynaspin project (Grant No. FMRX-CT97-0124).

[1] J. S. Moodera, L. R. Kinder, T. M. Wong, and R. Meservey, Phys. Rev. Lett. **74**, 3273 (1995).
[2] V. da Costa, C. Tiusan, T. Dimopoulos, and K. Ounadjela, Phys. Rev. Lett. **85**, 876 (2000).
[3] H. A. M. van den Berg, W. Clemens, G. Gieres, G. Rupp, M. Vieth, J. Wecker, and S. Zoll, J. Magn. Magn. Mater. **165**, 524 (1997).
[4] C. Tiusan, T. Dimopoulos, K. Ounadjela, M. Hehn, H. A. M. van den Berg, Y. Henry, and V. Da Costa, Phys. Rev. B **61**, 580 (2000).
[5] J. H. Greiner, J. Appl. Phys. **42**, 5151 (1971).
[6] J. Nassar, M. Hehn, A. Vaures, F. Petroff, and A. Fert, Appl. Phys. Lett. **73**, 698 (1998).